

Photocatalytic paper using zinc oxide nanorods

Sunandan Baruah, Mayuree Jaisai, Reza Imani¹, Mousa M Nazhad and Joydeep Dutta

Center of Excellence in Nanotechnology, School of Engineering and Technology, Asian Institute of Technology, Klong Luang, Pathumthani 12120, Thailand

E-mail: joy@ait.asia

Received 12 July 2010

Accepted for publication 28 September 2010

Published 29 November 2010

Online at stacks.iop.org/STAM/11/055002

Abstract

Zinc oxide (ZnO) nanorods were grown on a paper support prepared from soft wood pulp. The photocatalytic activity of a sheet of paper with ZnO nanorods embedded in its porous matrix has been studied. ZnO nanorods were firmly attached to cellulose fibers and the photocatalytic paper samples were reused several times with nominal decrease in efficiency. Photodegradation of up to 93% was observed for methylene blue in the presence of paper filled with ZnO nanorods upon irradiation with visible light at 963 W m^{-2} for 120 min. Under similar conditions, photodegradation of approximately 35% was observed for methyl orange. Antibacterial tests revealed that the photocatalytic paper inhibits the growth of *Escherichia coli* under room lighting conditions.

Keywords: zinc oxide, nanorod, paper, photocatalysis, antimicrobial, hydrothermal

1. Introduction

Paper is widely used for a variety of applications such as writing, printing, packaging, cleaning, construction and decoration. To further broaden the utility of paper and other nonwoven cellulosic materials, specialty paper was developed targeting specific applications like chromatography, filtration and printing, to name a few. These added functionalities in paper are achieved through different coating technologies. Paper is coated with different compounds to impart qualities like improved surface gloss and smoothness or lower ink absorbency. Photocatalytic paper is a type of specialty paper that was developed to degrade organic pollutants and immobilize microbes [1]. This type of antimicrobial and antifouling paper can have wide applications in health-related activities.

Photocatalysis with different semiconducting metal oxide nanoparticles has been an active area of research following the successful demonstration of the photolysis of water using a titania (TiO_2) photoanode [2]. Zinc oxide (ZnO), with its high surface reactivity owing to its large number of active surface

defect states, has emerged as a more efficient photocatalyst than TiO_2 . It has high reaction and mineralization rates [3] because of its more efficient hydroxyl ion generation [4]. ZnO can be structurally modified for visible light absorption paving the way for visible-light photocatalytic activity [5]. Furthermore, Zn^{2+} ions originating from slow dissolution of ZnO in moist environments can immobilize microbes [6]. As the surface area and surface defects play an important role in the photocatalytic activity of metal oxide nanostructures, one-dimensional nanostructures like nanowires/nanorods are ideal candidates for application to photocatalysis since they offer a larger surface-to-volume ratio than nanoparticulate thin films [5].

Photocatalysis using suspended nanoparticles to remove contaminants in a liquid is an efficient process, but the subsequent removal of the nanoparticles from the liquid can be cumbersome and adds an extra process step. It is therefore important that nanoparticulate photocatalysts should be attached to a support, as freely suspended nanoparticles can enter the human body through skin pores and may lead to health-related problems. Pozzo *et al* [7] have also discussed the importance of catalyst supports and opined that there is an inverse relationship between the adhesion of a catalyst to a support and its photocatalytic activity. There are only a few

¹ Now at: Wood and Paper Department, Islamic Azad University, Tehran, Iran.

reports (including patents) on the use of paper as a catalyst support [1, 4, 8, 9].

Photocatalytic paper was first reported by Matsubara *et al* [10] in 1995, who presented the catalytic degradation of acetaldehyde in the vapor phase using illumination with a weak fluorescent light. Subsequently, a few publications and patents describing photocatalytic paper have appeared in the literature [11–13]. The majority of available reports on photocatalytic paper mention TiO_2 as a photocatalyst, which absorbs light mostly in the ultraviolet region of the electromagnetic spectrum [7]. Ghule *et al* [14] reported the growth of ZnO nanoparticulate coating on paper support and studied its antibacterial property. ZnO nanorods, which can be strongly attached to any type of substrates through proper surface treatment before seeding [15], are an attractive option for photocatalytic applications. This work is one of the first reports on the *in situ* growth of ZnO nanorods on a cellulose support with target application as a visible-light photocatalyst.

2. Experimental details

2.1. Procedure for preparing photocatalytic paper

In a typical process, 30 g of dry bleached kraft soft wood pulp was chopped and dipped in water for 4 h, and the volume of the pulp suspension was increased up to 2000 ml using water (consistency of suspension of 1.5%). The suspension was then disintegrated at a rotation speed of 30 000 rpm using a scan-C 18:65 standard. After disintegration, water was removed from the fiber suspension using a Buchner funnel. For refining, the consistency of the pulp was adjusted at 10%. Pulp was refined using a PFI mill based on scan-C 24:67 standard at 10 000 rpm. To make hand sheets, pulp suspensions were diluted to about 0.2% by adding 15 000 ml of water to 30 g of refined pulp. After dewatering using a FORMAX standard sheet mold, a fiber suspension with a consistency of approximately 0.2% was obtained. A circular sheet was made using a scan-C 24:76 standard with a diameter of 15.9 cm and a basis weight of 35 g m^{-2} . Photocatalytic paper was prepared through a subsequent post-treatment process, which is normally referred to as 'size press treatment' in papermaking. The thus-prepared sheets were seeded with ZnO nanoparticles through dip coating. They were dipped three times and dried at 90°C for 15 min after each dipping. The ZnO nanorods were then grown following the procedure detailed in section 2.3.

2.2. Synthesis of ZnO seed nanoparticles

ZnO nanoparticles were synthesized in a colloidal solution using ethanol as the solvent following the procedure reported in [16, 17]. Briefly, 40 ml of 2 mM zinc acetate dihydrate $[(\text{CH}_3\text{COO})_2\text{Zn} \cdot 2\text{H}_2\text{O}$, Merck] solution was heat-treated at 70°C for 0.5 h; 20 ml of 4 mM sodium hydroxide (NaOH, Merck) solution was then added dropwise, and the admixture was hydrolyzed for 2 h at 60°C .

2.3. Growth of ZnO nanorods

ZnO nanorods were grown using a simple and efficient hydrothermal growth process [18]. Paper sheets were initially seeded by dipping in a colloidal dispersion of ZnO nanoparticles and dried at 90°C . They were then dipped in an equimolar solution of zinc nitrate hexahydrate $[\text{Zn}(\text{NO}_3)_2 \cdot 6\text{H}_2\text{O}$, APS Ajax Finechem] and hexamethylenetetramine $[(\text{CH}_2)_6\text{N}_4$, Carlo Erba] and maintained at 90°C for 10 h. Two different concentrations of zinc nitrate and hexamine were used for the nanorod growth: samples 1 (20 mM) and 2 (10 mM). The nanorods grew out of the seeds preferentially along the *c*-axis of the wurtzite structure [17]. The reaction bath was replenished after 5 h [5]. The sheets were then removed and washed with deionized water several times and dried at 70°C for 6 h. Nanorod dimensions were quantified using Scion image processing software applied to scanning electron microscopy (SEM) images. The images were obtained with a JEOL JSM-6301F microscope operated at 20 kV. Transmission electron microscopy (TEM) images were taken with a JEOL/JEM 2010 microscope operated at 120 kV.

It is important that a catalyst should remain firmly attached to the support (paper in this case) and that its activity should be repeatable. A simple experiment was carried out to determine whether the ZnO nanorods were firmly attached to the paper. Square sheets ($1 \times 1 \text{ cm}^2$) of untreated paper and treated paper were air-blown at a pressure of 2 bar. Changes in their weight were monitored to assess the removal of the ZnO nanorods from the paper support.

2.4. Photocatalysis tests

2.4.1 Organic dyes Photocatalysis was studied using two test contaminants, methylene blue (MB, $\text{C}_{16}\text{H}_{18}\text{N}_3\text{SCl}$, Carlo Erba) and methyl orange (MO, $\text{C}_{14}\text{H}_{14}\text{N}_3\text{NaO}_3\text{S}$, Carlo Erba). The photodegradation of MB results in the formation of leuco methylene blue ($\text{C}_{16}\text{H}_{19}\text{N}_3\text{S}$) [19], while that of MO produces hydrazine (N_2H_4) and some other reaction intermediates, leading to a change in optical absorption [20]. Solutions of the test contaminants ($10 \mu\text{M}$) were prepared in deionized water and put in polymethyl methacrylate (PMMA) cuvettes together with a rectangular piece of photocatalytic paper ($3 \times 1 \text{ cm}^2$). The cuvettes were then placed in front of a 500 W halogen lamp. A glass tank filled with water was installed between the lamp and the cuvettes to absorb UV light and infrared light. The incident light intensity was measured with a Kipp and Zonen pyranometer as 963 W m^{-2} . Similar cuvettes containing the dyes and untreated paper samples were used as controls. Optical absorption spectra were recorded upon light irradiation at different time intervals using an Ocean Optics spectrophotometer to monitor the rate of decolorization of the test contaminants. The degradation of the dye was estimated in terms of the change in absorption at $\lambda_{\text{max}} \sim 665 \text{ nm}$ for MB and at $\lambda_{\text{max}} \sim 460 \text{ nm}$ for MO.

The degradation efficiency was calculated using

$$\begin{aligned} \text{Efficiency (\%)} &= [(I_0 - I)/I_0] \times 100 \\ &= [(C_0 - C)/C_0] \times 100 \end{aligned} \quad (1)$$

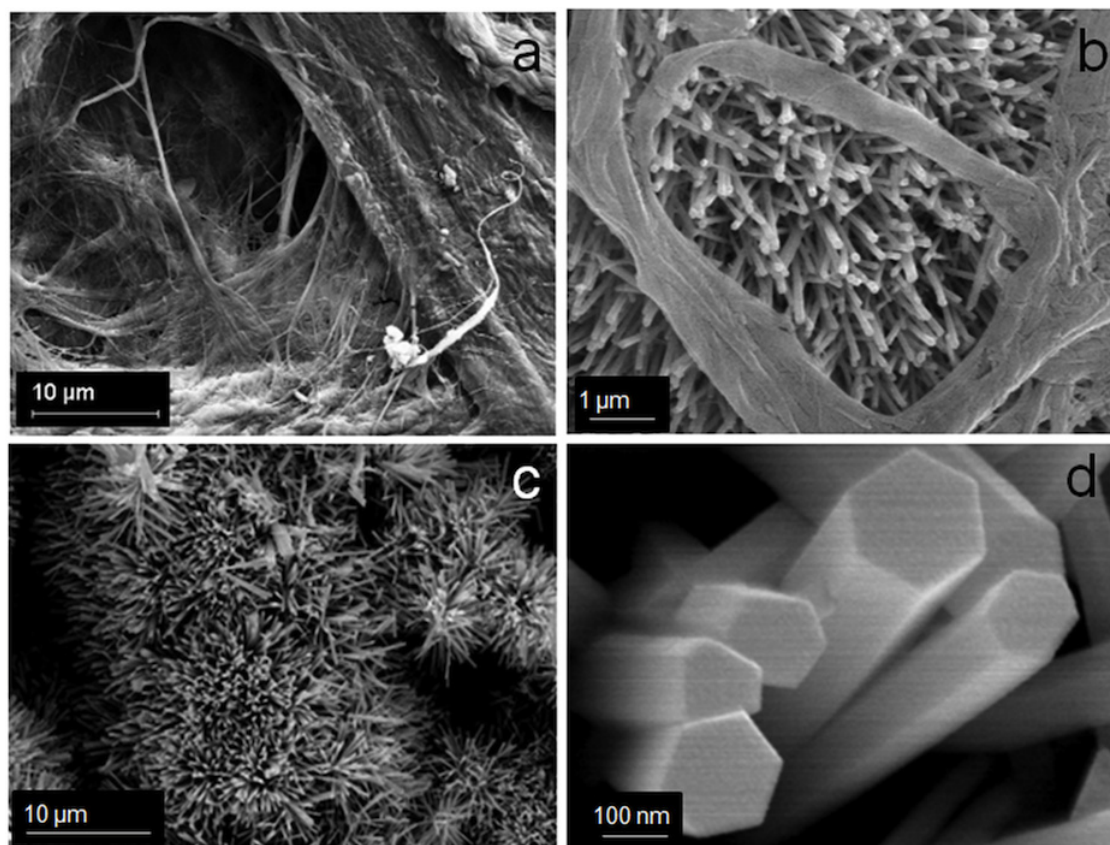


Figure 1. Scanning electron micrographs showing (a) porous structure of the paper, (b) ZnO nanorods growing in the paper pores, (c) ZnO nanorods on the top surface of the paper and (d) close up view of the ZnO nanorods.

where I_0 is the initial absorption intensity of MB at $\lambda_{\max} = 665$ nm or of MO at $\lambda_{\max} = 460$ nm, I is the intensity at λ_{\max} after illumination at time t , C_0 is the initial concentration of the dyes and is C the concentration after illumination at time t . The photocatalytic tests with MB and MO dyes were repeated after rinsing the used photocatalytic paper with deionized water and drying at it 70 °C.

2.4.2 Antibacterial activity. The microbicidal property of the photocatalytic paper was monitored using commonly available strains of the bacterium *Escherichia Coli* (*E. coli*), some of which can cause severe food poisoning in humans [21]. Wild-type *E. coli* (TISTR 073) cells were cultivated on nutrient agar (source) and incubated at 37 °C for 18 h using the streak plate method [22]. After harvesting the cells incubated for 18 h by scraping from the nutrient agar, they were mixed in phosphate buffered saline by a vortex mixer until they were uniformly dispersed. Then the suspension was centrifuged at 4000 rpm for 10 min and the supernatant was discarded. This process was repeated twice and the cell pellet was mixed with 1 ml of deionized water for the experiments. The *E. coli* cells thus prepared were redispersed in 10 ml of Milli-Q water, and the optical density of the suspension was kept at 0.6 (600 nm wavelength) for all the tests.

To observe antibacterial activity, three sheets ($1.5 \times 1.5 \text{ cm}^2$) of both the untreated paper and ZnO-treated paper

were taken and dried for 10 min in a laminar airflow. Antibacterial activity was assessed via the zone of inhibition, i.e. the absence of viable *E. coli* cells, around the paper samples. For this purpose, 100 μ of *E. coli* cell suspension was spread on nutrient agar, and the square paper samples were placed on it in a triangular formation. The temperature inside the incubation box was maintained at 37 °C and incubation was continued for 72 h. The area of inhibition surrounding the square paper samples of 2.25 cm² area was then measured. *E. coli* cells were stained with safranin dye before imaging. Photocatalysis tests were carried out under illumination using a tungsten halogen lamp (light intensity $\sim 11 \text{ W m}^{-2}$ on the sample) and also in the dark as a control.

3. Results and discussion

The porous (void) structure of paper prepared from cellulose pulp is attractive as a catalyst support as it allows higher loading of photocatalysts. The enhanced decomposition of volatile organic compounds as a result of the increased porosity of paper has been reported in the literature [23] An SEM image of as-prepared paper is shown in figure 1(a) where a porous structure can be observed. The process of affixing presynthesized ZnO nanoparticles in colloidal form allows nanoparticles to percolate through gaps of porous cellulose. As a result, ZnO nanorods grow even deep inside the pores, thereby increasing loading in a sample. ZnO nanorods grown

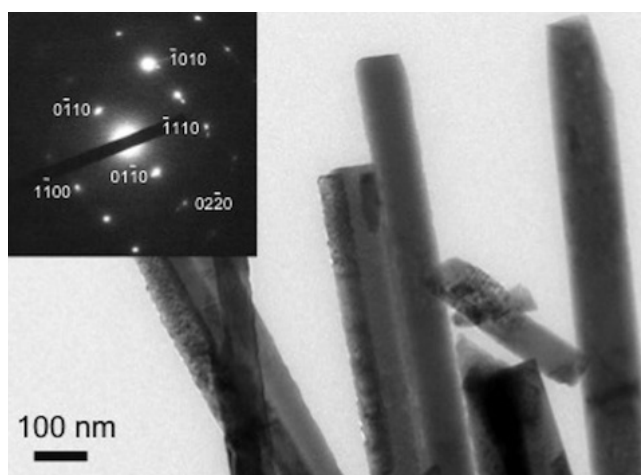


Figure 2. Transmission electron micrograph showing a section of a ZnO nanorod cluster. Inset: electron diffraction pattern from one ZnO nanorod.

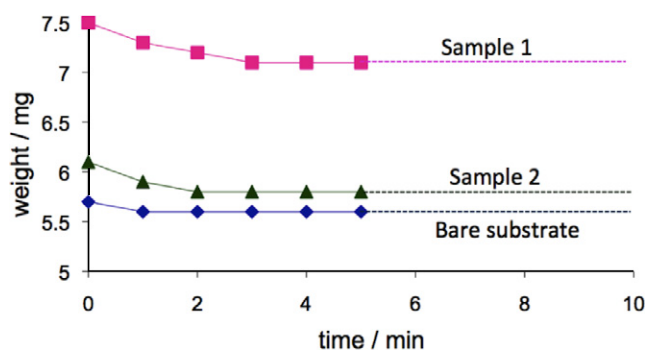


Figure 3. Weight loss of $1 \times 1\text{cm}^2$ paper samples with ZnO nanorods (samples 1 and 2) and without ZnO (untreated) after blowing air at a pressure of 2 bar. The weight loss is plotted as a function of time of air blowing. The weight of the samples became almost constant after 2 min of blowing indicating the firm attachment of the ZnO nanorods.

inside a porous structure of paper can be seen in figure 1(b). Figure 1(c) shows ZnO nanorods on the top surface of the paper, and figure 1(d) shows a close-up view of the ZnO nanorods. Measurements carried out on twenty samples revealed the width and length of the nanorods for sample 1 as 260 and 2000 nm, and the corresponding values for sample 2 as 80 and 600 nm, respectively. A TEM image of the ZnO nanorods is shown in figure 2. The nanorods are highly crystalline, having the wurtzite structure, as is evident from the electron diffraction pattern shown in the inset of figure 2. The diffraction pattern could be indexed to different planes of the wurtzite structure. The formation of wurtzite under hydrothermal growth conditions and the presence of inherent structural defects were also observed by Morin *et al* [24] using TEM and electron diffraction analysis. The wurtzite structure is ideal for hydrothermal anisotropic growth owing to the presence of polar and non-polar surfaces, with a natural tendency to minimize the polar surface in order to reduce surface energy [18].

The attachment of the ZnO nanorods to the cellulose support is important for preventing the removal of

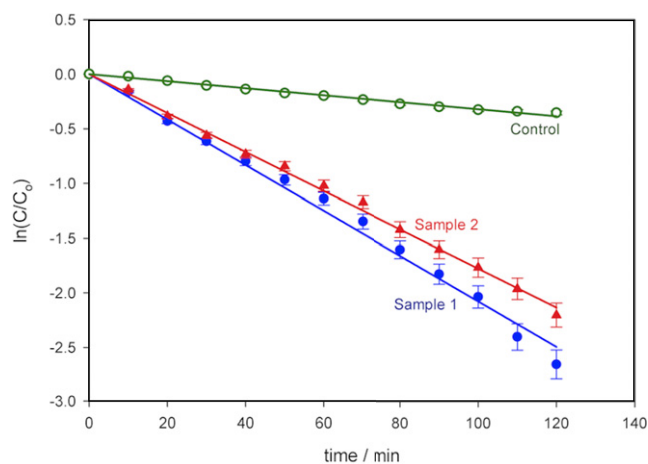


Figure 4. Photodegradation of MB using photocatalytic paper with ZnO nanorods of different dimensions (samples 1 and 2). Sample 1 with thicker and longer nanorods showed higher photoreactivity (93% degradation after 120 min) than sample 2 (89% degradation after 120 min). The control sample of paper without ZnO nanorods showed 30% degradation in 120 min. Light intensity at the sample: 963 Wm^{-2} , error bar: 5%.

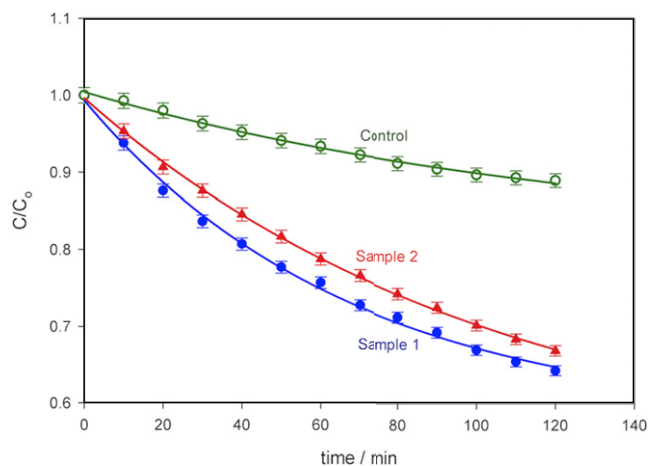


Figure 5. Photodegradation of MO using photocatalytic paper with ZnO nanorods of different dimensions (samples 1 and 2). Sample 1 with thicker and longer nanorods showed higher photoreactivity (35% after 120 min) than sample 2 (30% in 120 min). The control paper sample without ZnO nanorods showed 11% degradation in 120 min. Light intensity at the sample: 963 Wm^{-2} , error bar: 1%.

nanostructures from the test solution. The air blowing experiment detailed in section 2.3 revealed that after an initial weight loss, the sample weight stabilized (figure 3). The initial weight loss can be attributed to the removal of loosely bound ZnO agglomerates and cigarlike structures resulting from secondary growth [18], which were not removed by washing. The slight decrease in the weight of the bare substrate is due to the removal of broken bits of fibers resulting from the cutting process. All the photocatalysis experiments reported below were carried out after blowing air onto the samples at a pressure of 2 bar for 10 min.

Figure 4 shows the results of the photodegradation of MB using the photocatalytic paper with ZnO nanorods (samples 1 and 2). As reported in [25], the degradation of MB is

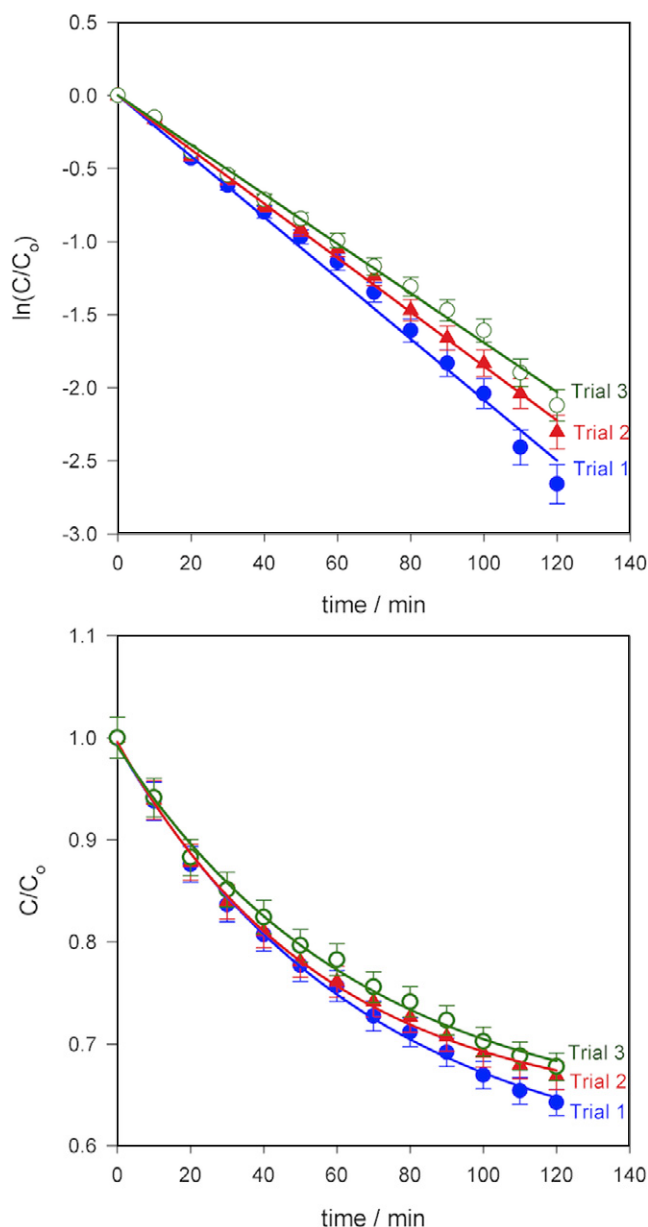


Figure 6. Repeatability test on the photocatalytic paper (sample 1) on (a) MB and (b) MO. Degradation efficiency of MB decreased by approximately 3.2% in the second trial and 5.4% in the third trial (error bar: 5%). The corresponding values for MO were 6.4% and 13%. Light intensity at the sample: 963 Wm^{-2} , error bar: 2%.

exponential with time. The degradation rate constant k for MB was obtained from the semi-logarithmic plot in figure 4 using

$$\ln(C/C_0) = -kt \quad (2)$$

The degradation rate constants are comparable for both the samples with decomposed MB fractions of 93% ($k \sim 0.0208 \text{ min}^{-1}$, sample 1) and 89% ($k \sim 0.0178 \text{ min}^{-1}$, Sample 2) upon illumination for 120 min. During this period, the control ($10 \mu\text{M}$ MB solution only) degraded by 30% ($k \sim 0.0032 \text{ min}^{-1}$).

The photocatalytic degradation of MO is also exponential, as reported in [26, 27]. Our observations of

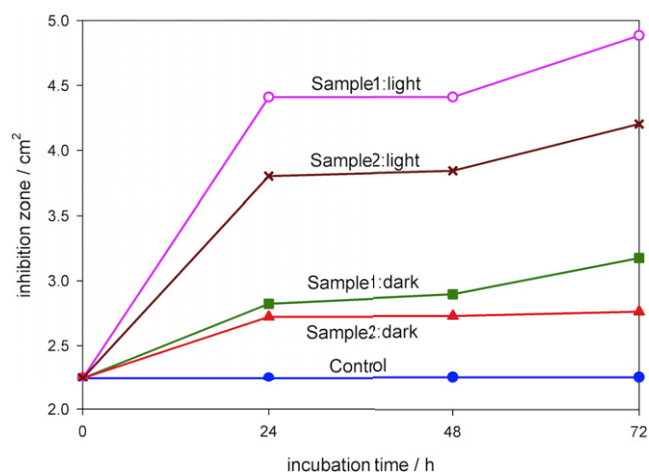


Figure 7. Increase in zone of inhibition for *E. coli* upon incubation in the dark and under illumination in the presence of photocatalytic paper. No inhibition zone was observed for the control sample without ZnO nanorods. The antibacterial activity increased by almost threefold upon illumination with a tungsten halogen lamp at an intensity of only 11 Wm^{-2} at the sample position. The activity in the dark is due to the bactericidal properties of zinc oxide.

the degradation of MO using the photocatalytic paper could be fitted with equation (3), and the degradation rate constants were calculated using equation (4).

$$C/C_0 = y_0 + ae^{-bt} \quad (3)$$

$$\ln(C/C_0 - y_0) = -kt \quad (4)$$

The degradation of MO is shown in figure 5 as a plot of C/C_0 versus time of illumination. The decomposed fraction of MO was much lower (between 30 and 35% in 120 min) than that of MB. The rate constants (k) for MO are calculated as 0.0067 min^{-1} for sample 1, 0.0046 min^{-1} for sample 2 and 0.0015 min^{-1} for the control.

A repeatability test was carried out three times using sample 1 for both MB and MO and the results are shown in figure 6. The reductions in MB degradation efficiency after 120 min of exposure to visible light were $\sim 3.2\%$ for the second trial and $\sim 5.4\%$ for the third trial, and the rate constants were 0.0185 and 0.0169 min^{-1} , respectively. The corresponding values for MO were 6.4%, 13%, 0.0064 and 0.0055 min^{-1} . The decrease in efficiency is probably due to the photodegradation product molecules that did not desorb during the washing process thereby decreasing the number of active sites on the surface. The desorption of the molecules on the ZnO nanorod surfaces by changing the pH of the solution, for example, should lead to a better repeatability.

Figure 7 shows the results of the antimicrobial tests with *E. coli* as a graph showing a comparison of the inhibition zone surrounding the paper sample for different conditions. Experiments were carried out in the dark as a control since ZnO itself is a bactericidal material. In moist environments, ZnO undergoes a slow dissolution and releases Zn^{2+} ions [28]. Zn^{2+} ions can rupture the bacterial cell wall [29] and can move inside bacterial cells, thereby inhibiting their growth [6]. Cho *et al* [30] reported the inhibition of *E. coli*

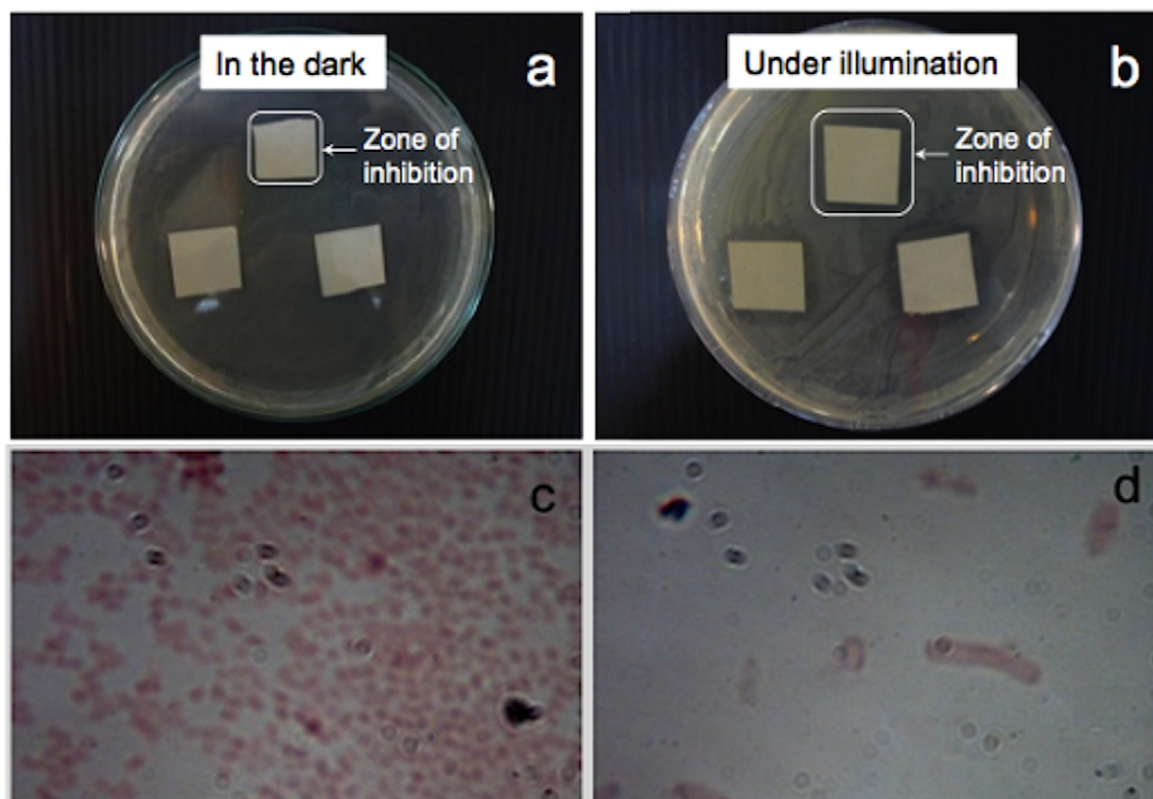


Figure 8. Results of antibacterial experiments carried out using photocatalytic paper (Sample 1) after incubation for 48 h (a) in the dark and (b) under illumination with a tungsten halogen lamp. The inhibition zone increased from $1.7 \times 1.7 \text{ cm}^2$ in the dark to $2.1 \times 2.1 \text{ cm}^2$ under visible-light illumination. Optical images taken at a magnification of $1000\times$ (c) outside the inhibition zone and (d) inside the inhibition zone.

growth in the presence of Zn^{2+} ions, and the use of ZnO nanoparticles to suppress the growth of *Streptococcus mutans*, a gram-positive bacterium, in the dark was documented in [31]. The increase in the inhibition zone upon illumination with visible light is indicative of photocatalytic immobilization. Free electrons from electron-hole pairs generated by the illumination of ZnO can be injected into a bacterium and rupture its cell wall [32]. Not only do bacteria become immobilized on the surface of photocatalytic paper but they also cannot survive in the vicinity of ZnO-treated paper. No inhibition was observed in either the dark or illuminated condition for the control sample (paper with no ZnO nanorods) indicating the lack of microbicidal property of the paper. Figure 7 indicates that an inhibition zone could be observed for both samples 1 (3.2 cm^2) and 2 (2.8 cm^2) after incubation for 72 h in the dark. This zone increased upon illumination to 4.9 cm^2 (sample 1) and 4.2 cm^2 (sample 2) as a result of the photocatalytic activity of the ZnO nanorods. After a 24 h incubation under illumination, the inhibition zones were 4.4 cm^2 for sample 1 and 3.8 cm^2 for sample 2. The inhibition zones can be clearly observed in the digital photographs in figure 8 showing sample 2 after incubation for 48 h in the dark and under illumination from a tungsten halogen lamp. Images of the bacterial cells viewed under an optical microscope at a magnification of $1000\times$ inside and outside the zone of inhibition are shown in figures 8(c) and (d), respectively.

4. Conclusions

ZnO nanorods have been successfully grown in paper supports and their photocatalytic activity was determined. The efficient photodegradation of organic dyes (methylene blue and methyl orange) and the photocatalytic immobilization of common bacterium, *E. coli*, were studied under visible-light irradiation. A 93% photodegradation was observed for methylene blue and a 35% photodegradation was observed for methyl orange in the presence of the photocatalyst paper upon white-light irradiation at 963 Wm^{-2} . Repeatability tests showed that the photocatalytic paper could be reused several times with a nominal decrease in efficiency. Antibacterial tests revealed that the photocatalytic paper is capable of completely eliminating *E. coli* in its vicinity even under room lighting condition.

Acknowledgments

The authors would like to acknowledge partial financial support from the National Nanotechnology Center, of the National Science and Technology Development Agency (NSTDA), Ministry of Science and Technology (MOST), Thailand and the Centre of Excellence in Nanotechnology at the Asian Institute of Technology, Thailand.

References

- [1] Pelton R, Geng X and Brook M 2006 *Adv. Colloid Interface Sci.* **127** 43
- [2] Fujishima A and Honda K 1972 *Nature* **238** 37
- [3] Poullos I, Makri D and Prohaska X 1999 *Global Nest: The Int. J.* **1** 55
- [4] Carraway E R, Hoffman A J and Hoffmann M R 1994 *Environ. Sci. Technol.* **28** 786
- [5] Baruah S, Rafique R F and Dutta J 2008 *Nano* **3** 8
- [6] Cho Y H, Lee S J, Lee J Y, Kim S W, Lee C B, Lee W Y and Yoon M S 2002 *Int. J. Antimicrob. Agents* **19** 576
- [7] Pozzo R L, Baltanas M A and Cassano A E 1997 *Catal. Today* **39** 219
- [8] Okazaki M 2000 *Kinoshi Kenkyu Kaishi* **38** 93
- [9] Aguedach A, Brosillon S, Morvan J and Lhadi E K 2005 *Appl. Catal. B* **57** 55
- [10] Matsubara H, Takada M, Koyama S, Hashimoto K and Fujishima A 1995 *Chem. Lett.* **9** 767
- [11] Iguchi Y, Ichiura H, Kitaoka T and Tanaka H 2003 *Chemosphere* **53** 1193
- [12] Koga K, Kawakatsu H and Sakamoto T 1999 *Kenkyu Hokoku-Fukuoka-ken Kogyo Gijutsu Senta* **9** 63
- [13] Raillard C, Haquet V, Le Cloirec and Legrand J 2004 *J. Photochem. Photobiol. A* **163** 425
- [14] Ghule K, Ghule A V, Chen B J and Ling Y C 2006 *Green Chem.* **8** 1034
- [15] Baruah S, Thanachayanont C and Dutta J 2008 *Sci. Technol. Adv. Mater.* **9** 025009
- [16] Ullah R and Dutta J 2008 *J. Hazard. Mater.* **156** 194
- [17] Sugunan A, Warad H C, Boman M and Dutta J 2006 *J. Sol-Gel Sci. Technol.* **39** 49
- [18] Baruah S and Dutta J 2009 *Sci. Technol. Adv. Mater.* **10** 013001
- [19] www.udel.edu/pchem/C446/Experiments/exp7.pdf
- [20] Quintana M, Ricra E, Rodriguez J and Estrada W 2002 *Catal. Today* **76** 141
- [21] Vogt R L and Dippold L 2005 *Public Health Reports* **120** 174
- [22] Soper R 2005 *Biological Science* (Cambridge: Cambridge University Press)
- [23] Fukahori S, Iguchi Y, Ichiura H, Kitaoka T, Tanaka H and Wariishi H 2007 *Chemosphere* **66** 2136
- [24] Morin S A, Bierman M J, Tong J and Jin S 2010 *Science* **328** 476
- [25] Xu N, Shi Z, Fan Y, Dong J, Shi J and Hu M Z C 1999 *Ind. Eng. Chem. Res.* **38** 373
- [26] Chen J Q, Wang D, Zhu M X and Gao C J 2006 *J. Hazard. Mater.* **138** 182
- [27] Xu J C, Lu M, Guo X Y and Li H L 2005 *J. Mol. Catal. A: Chem.* **226** 123
- [28] Han J, Qiu W and Gao W 2010 *J. Hazard. Mater.* **178** 115
- [29] Atmaca S, Gul K and Clcek R 1998 *Turk. J. Med. Sci.* **28** 595
- [30] Cho Y H, Lee S J, Lee J Y, Kim S W, Lee C B, Lee W Y and Yoon M S 2002 *Int. J. Antimicrob. Agents* **19** 576
- [31] Hernandez-Sierra J F, Ruiz F, Cruz Pena, Martinez-Gutierrez F, Martinez A E, de Jesus, Pozos Guillen, Tapia-Perez H and Martinez Castanon G 2008 *Nanomed. Nanotechnol. Biol. Med.* **4** 237
- [32] Huang Z, Maness P C, Blake D M, Wolfrum E J, Smolinski S L and Jacoby W A 2000 *J. Photochem. Photobiol. A* **130** 163